

# High Temperature Deformation Behaviour and Dislocation Substructure of Impacted Inconel 625 Alloy

Woei-Shyan Lee \* and Chien-Wei Huang\*\*

**Keywords** : Hopkinson bar, Inconel 625 alloy, high temperature deformation, high strain rate, dislocation density

## ABSTRACT

The dynamic impact response and dislocation characteristics of Inconel 625 alloy are investigated under strain rates ranging from 3700 to 6400 s<sup>-1</sup> and temperatures of 25°C, 300°C and 750°C, respectively, using a compressive split-Hopkinson pressure bar. The results show that the flow response is sensitive to both the temperature and the strain rate. For a constant temperature, the yield strength, material constant and work hardening coefficient all increase with increasing strain rate. However, for a constant strain rate, the yield strength, material constant and work hardening coefficient all reduce with increasing temperature. The flow stress corresponding to a true strain of 0.35 can be described by a power law relation with an activation energy of 2.04 kJ/mol and an average strain rate sensitivity of 0.61. Moreover, the stress and temperature dependence of the strain rate is adequately described by the Zener-Hollomon parameter. Transmission electron microscopy (TEM) observations show that the dislocation density increases with increasing strain rate, but decreases with increasing temperature. The dislocation density and work hardening stress are related by the Bailey-Hirsch equation  $\sigma = \sigma_0 + \alpha_1 G b \sqrt{\rho}$ , with  $\alpha_1$  equal to 0.316.

## INTRODUCTION

Inconel 625 is a nickel-based super alloy strengthened mainly by the solid-solution hardening effect of “niobium and molybdenum in a nickel-

chromium matrix [1]. The alloy finds widespread use in the aerospace, chemical, petrochemical and marine industries due to its good yield strength, fatigue strength, fabrication ability (including joining), and corrosion resistance [2]. Inconel 625 alloy is a crucial material in nuclear power plant components and is widely used in the fabrication of light-water reactors (LWRs) and supercritical water reactors (SCWRs) [3, 4]. However, although many studies have been reported on Inconel 625 in the literature, the high strain rate deformation behaviour of Inconel 625 is still unclear. Consequently, further investigation into the mechanical deformation behaviour of Inconel 625 alloy at high temperatures and high strain rates is required.

The macroscopic and microscopic response of engineering materials under high strain-rate loading is critically dependent on the strain rate, temperature and microstructure. Previous studies have shown that the flow stress and dislocation density generally increase with increasing strain rate, but decrease with increasing temperature [5,6]. However, polycrystalline face-centred cubic (fcc) metals exhibit different hardening mechanisms depending on the strain rate and deformation temperature. For engineering metals and alloys, the high temperature creep strain is conveniently modelled using the Zener-Hollomon parameter [7], defined as

$$Z = \dot{\epsilon} \exp(Q / RT) \quad (1)$$

where  $\dot{\epsilon}$  is the strain rate,  $Q$  is the activation energy of the mechanism controlling the deformation rate,  $R$  is the universal gas constant and  $T$  is the absolute temperature. For deformation with low  $Z$  values (i.e., low strain rate and high temperature), deformation is dominated by dislocation activity. By contrast, for high  $Z$  values, deformation occurs primarily as a result of plastic deformation [8, 9].

The present study uses a compressive split-Hopkinson pressure bar (SHPB) to investigate the effects of the strain rate and temperature on the flow response and dislocation evolution of Inconel 625 alloy at strain rates of 3700 to 6400 s<sup>-1</sup> and temperatures of 25°C, 300°C and 750°C. The relationship between the flow stress and the

*Paper Received July, 2019. Revised August, 2019, Accepted August, 2019, Author for Correspondence: Woei-Shyan Lee.*

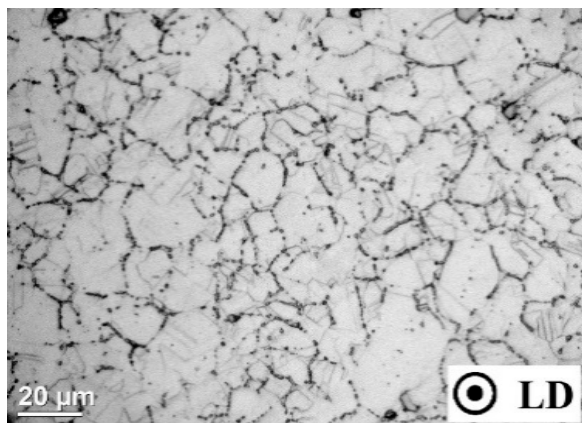
\* Distinguished Professor, Department of Mechanical Engineering, National Cheng Kung University, Tainan, Taiwan 70101, ROC.

\*\* Graduate Student, Department of Mechanical Engineering, National Cheng Kung University, Tainan, Taiwan 70101, ROC.

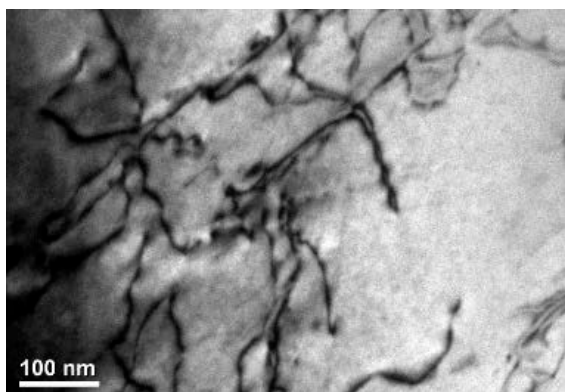
dislocation density is clarified in terms of the strain rate and temperature conditions by means of transmission electron microscopy (TEM) observations.

## MATERIALS AND METHODS

The Inconel 625 alloy used in the present study was purchased from S-Tech Corp, Taiwan. According to the manufacturer's specification, the as-received alloy had a composition (wt%) of 21.1% Cr, 8.3% Mo, 4.1% Fe, 3.5% Nb, 0.36% Ti, 0.21% Al, 0.20% Si, 0.05% Co, 0.04% C, 0.03% Mn, 0.01% Cu, and a balance of Ni. Cylindrical specimens with a length and diameter of 7 mm were machined from the as-received bars with a tolerance of  $\pm 0.01$  mm using an electro-discharge machine (EDM). Figure 1(a) presents an optical micrograph of the as-received alloy. The microstructure consists of equiaxed grains and annealing twins, which are typical of this Inconel 625 alloy. Furthermore, the matrix and grain boundaries contain  $M_{23}C_6$  and MC carbide precipitates. Figure 1(b) presents a TEM micrograph of the dislocation structure of the as-received alloy. It is seen that the microstructure contains a relatively low number of dislocations.



(a)



(b)

Figure 1: (a)Optical micrograph; (b)TEM micrograph of as-received Inconel 625 alloy at room temperature.

The specimens were impacted at strain rates of 3700 s<sup>-1</sup>, 5000 s<sup>-1</sup> and 6400 s<sup>-1</sup> under temperatures of

25°C, 300°C and 750°C using a compressive split-Hopkinson pressure bar (SHPB) system [10]. The elevated deformation temperatures (300°C and 750°C) were obtained by enclosing the specimens in a clamshell radiant-heating furnace with an internal diameter of 25 mm and a heating element of length 300 mm. The temperature was monitored to within  $\pm 2^\circ\text{C}$  by means of a thermocouple attached to the specimen surface. To ensure frictionless impact conditions, the ends of the specimens were lubricated using commercial molybdenum disulfide (Molykote) mixed with a glass paste consisting of 80% PbO, 20% B<sub>2</sub>O<sub>3</sub> and alcohol. Finally, to compensate for the effects of the temperature gradient induced within the pressure bars of the SHPB system on the pulse reflections and elastic modulus, the original equations for the strain, strain rate and stress within the deformed specimens were modified to the forms shown in [11].

Following the impact tests, the microstructures of the Inconel 625 alloy specimens were examined by optical microscopy (OM), transmission electron microscopy (TEM) and energy dispersive spectroscopy (EDS). TEM thin foils were prepared by means of a twinjet thinning technique with a room-temperature electro-polishing solution of 10% HClO<sub>4</sub> / 90% C<sub>2</sub>H<sub>5</sub>OH and an agitation voltage of 15 V. The specimens were observed using a JEOL TEM-3010 device with an operating voltage of 300 kV. For each specimen, the dislocation density was calculated as  $\rho = 2N/Lt$  [12], when N is the average number of intersections between a dislocation and a random set of lines of length L, and t is the foil thickness.

## RESULTS AND DISCUSSIONS

### 3.1. Flow stress-strain response

Figures 2(a)~2(c) show the compressive true stress–strain curves of the Inconel 625 alloy specimens deformed at temperatures of 25, 300 and 750°C and strain rates of 3700, 5000 and 6400 s<sup>-1</sup>, respectively. In general, the results show that the flow stress increases with increasing strain rate, but decreases with increasing temperature. The flow stress and shape of the flow curves are strongly dependent on both the temperature and the strain rate. However, comparing the variations of the flow stress with the strain rate and temperature, respectively, it is found that the temperature has a greater effect on the flow stress than the strain rate. In particular, a pronounced softening effect occurs as the deformation temperature is increased. As for all metal alloys, the flow response of the present Inconel 625 alloy reflects different dislocation structures and

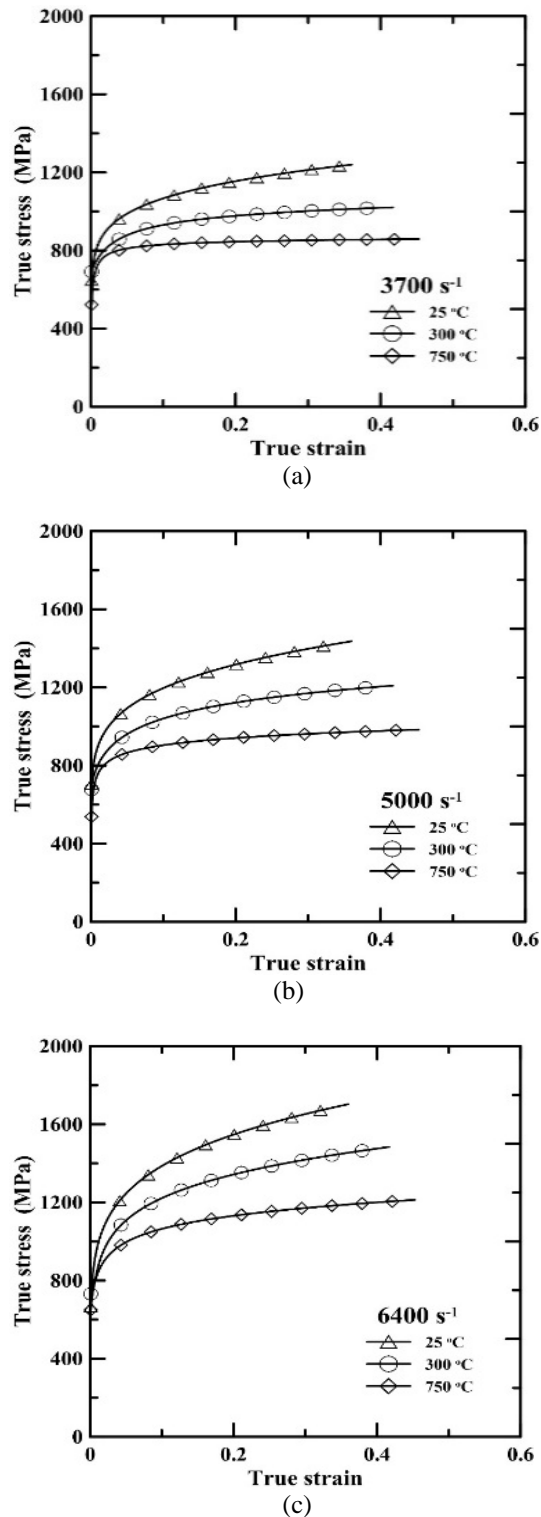


Figure 2: Stress-strain curves of Inconel 625 alloy deformed at temperatures of 25°C, 300°C and 750°C under strain rates of (a)  $3.7 \times 10^3 \text{ s}^{-1}$ , (b)  $5 \times 10^3 \text{ s}^{-1}$  and (c)  $6.4 \times 10^3 \text{ s}^{-1}$

degrees of mobility. For example, plastic deformation at high temperature promotes the movement of dislocations, whereas at high strain rates, dislocation activity is difficult. It is noted that none of the present

specimens fractured under the considered test conditions. Thus, it is inferred that Inconel 625 alloy has good ductility and strengthening properties under elevated temperatures and strain rates.

The flow stress-strain behaviour shown in Figs. 2(a)~2(c) can be further explored using a simple power law equation with the form  $\sigma = A + B\epsilon^n$ , where A is the yield strength, B is the material constant, and n is the work hardening coefficient. Table 1 shows the fitting results obtained for A, B and n for the current Inconel 625 alloy specimens under each of the considered temperatures and strain rate conditions. It is seen that for a given temperature, the yield strength, material constant and work hardening coefficient all increase with increasing strain rate. By contrast, for a given strain rate, the yield strength, material constant and work hardening coefficient all reduce as the temperature increases.

Table 1 Yield strength (A), material constant (B), and work hardening coefficient (n) of Inconel 625 alloy deformed at different strain rates and temperatures.

Temperature (°C)	Strain rate (s <sup>-1</sup> )	A (MPa)	B (MPa)	Work-hardening coefficient n
25	3700	479.3	1130.3	0.34
	5000	553.3	1398.8	0.41
	6400	648.7	1745.0	0.46
300	3700	446.7	732.1	0.22
	5000	538.3	886.2	0.28
	6400	621.9	1179.0	0.32
750	3700	364.6	572.7	0.12
	5000	520.8	554.7	0.18
	6400	601.3	747.0	0.22

### 3.2 Effects of strain rate and temperature

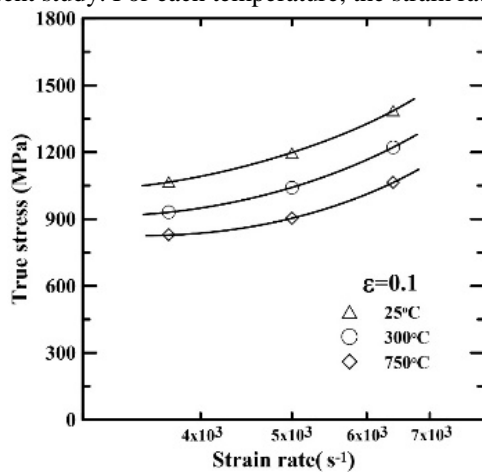
The stress-strain response curves in Figs. 2(a)-(c) show that the strain rate and temperature both play an important role in determining the mechanical properties and microstructures of Inconel 625 alloy. To clarify the effects of the strain rate and temperature on the dynamic response of the Inconel 625 specimens, Figs. 3(a) and 3(b) plot the true stress versus the logarithmic strain rate at true strains of 0.1 and 0.3, respectively. For both true strains and all three test temperatures, the flow stress increases with increasing strain rate. For each strain rate, the difference in the flow stress under the different test temperatures is

greater at a true strain of 0.3 than at a true strain of 0.1. However, for both true strains, the increase in the flow stress with increasing strain rate is less pronounced at the highest deformation temperature of 750°C. This can be attributed to a greater degree of dislocation annihilation and mobility at higher deformation temperatures. In other words, a higher deformation temperature increases the energy of the mobile dislocations and therefore improves their ability to overcome short-range barriers to motion during the deformation process.

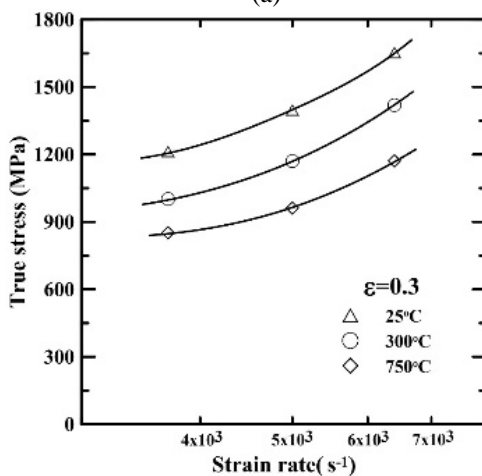
The strain rate behaviour of the present Inconel 625 alloy can be described by the following power law expression [13]:

$$\dot{\epsilon} = C_1 \sigma^n \exp(-Q/RT) \tag{2}$$

where  $Q$  is the effective activation energy required for deformation,  $R$  is the gas constant (8.314 J/mol K),  $T$  is the deformation temperature, and  $C_1$  and  $n$  are constants. Figure 4(a) shows the effect of the strain rate on the flow stress at a true strain of 0.35 for the three deformation temperatures considered in the present study. For each temperature, the strain rate



(a)



(b)

Figure 3: Effect of strain rate on true stress for true strains of (a) 0.1 and (b) 0.3 and temperatures of 25°C, 300°C and 750°C

sensitivity parameter (power law exponent), i.e.,

$$m = 1/n', \text{ can be determined by fitting with Eq. (2) as } \ln \sigma = Q/(n'RT) + (1/n') \ln \dot{\epsilon} - (1/n') \ln C_1. \tag{3}$$

For a given strain rate, the value of  $Q/n'$  in Eq. (3) can be obtained from the slope of the plot of  $\ln(\sigma)$  against the inverse temperature, as shown in Fig. 4(b) for the case of a true strain of 0.35. For the three strain rates considered in the present study, the average value of  $Q/n'$  is equal to 1.25 kJ/mol. Taking this value of  $Q/n'$  together with the stress-strain rate data presented in Fig. 4(a), the strain rate sensitivity parameter ( $m$ ) can be determined from Eq. (3) as 0.656, 0.599 and 0.577 for temperatures of 25°C, 300°C and 750°C, respectively. In other words, the strain rate sensitivity increases with decreasing temperature. Moreover, the average value of the strain rate sensitivity parameter is equal to 0.61, from which the average effective activation energy ( $Q$ ) for the current Inconel 625 alloy is found to be 2.04 kJ/mol.

The coupled effects of the strain rate and temperature on the deformation response can be evaluated by plotting the flow stress against the Zener-Hollomon parameter,  $Z (= \dot{\epsilon} \exp(Q/RT))$  [7]. Figure 4(c) shows the variation of the flow stress with  $Z$  for the present Inconel 625 alloy specimens for a constant true strain of 0.35. It is observed that the flow stress increases significantly with increasing  $Z$ . In other words, the maximum flow stress occurs at the lowest temperature and the highest strain rate. The significant increase in the flow stress at higher  $Z$  can be attributed to dislocation multiplication (the dominant mechanism), and is consistent with the strengthening effect shown in Fig. 3. From a detailed inspection, the results presented in Fig. 4(c) can be fitted using the following power law:

$$\sigma = AZ^m = 4.82Z^{0.61} \tag{4}$$

### 3.3 Dislocation substructure

Figures 5(a)–(f) present TEM images showing the dislocation substructures of the specimens deformed at 25°C, 300°C and 750°C and strain rates of 3700 s<sup>-1</sup> and 6400 s<sup>-1</sup>, respectively. It is seen that both the characteristics of the dislocations and their density are significantly affected by the strain rate and temperature, Table 2. In particular, for each test temperature, the dislocation density and degree of dislocation tangling increase with increasing strain rate.

Comparing Fig. 5(a) with 5(c) and 5(e) or Fig. 5(b) with 5(d) and 5(f), it is found that a higher strain rate prompts an increased number of dislocations and a reduced dislocation cell size. The higher dislocation density and reduced cell size constrain the mobility of the dislocations and therefore enhance the work hardening effect and resistance of the alloy to plastic deformation (see Fig. 2). However, for a constant strain rate, the dislocation density and the degree of dislocation tangling both decrease with an increasing

temperature. In other words, a high temperature prompts a thermal softening effect as a result of dislocation annihilation and rearrangement. Thus, as shown in Fig. 2, the strength of the present Inconel 625 alloy specimens reduces as the deformation temperature increases.

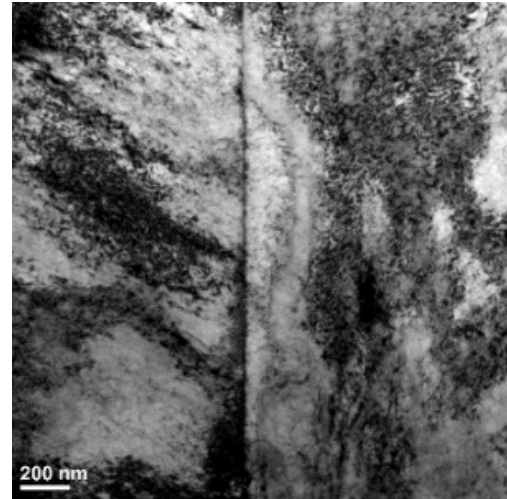
Table 2 Dislocation density of Inconel 625 alloy deformed at different strain rates and temperatures.

T (°C)	Strain rate(s <sup>-1</sup> )	Stress(MPa)	Dislocation density <sup>1/2</sup> (10 <sup>5</sup> cm <sup>-1</sup> )
25	3700	1256.06	13.3
	5000	1459.48	17.5
	6400	1733.01	21.3
300	3700	1018.86	11.6
	5000	1204.17	14.8
	6400	1475.50	16.8
750	3700	856.87	9.9
	5000	977.30	12.6
	6400	1200.14	14.4

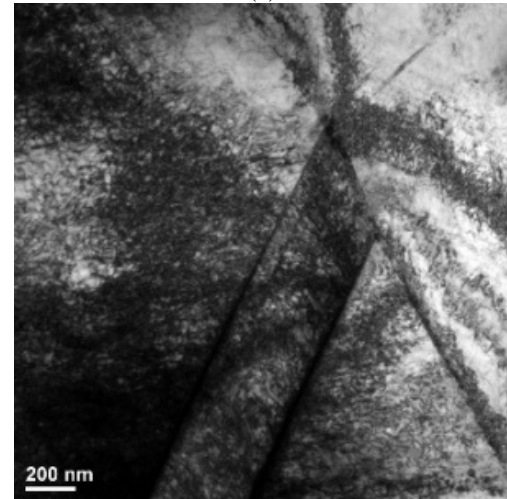
To further explore the correlation between the microstructural evolution of the Inconel 625 alloy specimens and their macroscopic behaviour, it is seen that the work hardening stress increases with an increasing dislocation density. For engineering metals and alloys, the square root of the dislocation density and the work hardening stress are related by the following Bailey-Hirsch equation [14]:

$$\sigma = \sigma_0 + \alpha G b \sqrt{\rho} \quad (5)$$

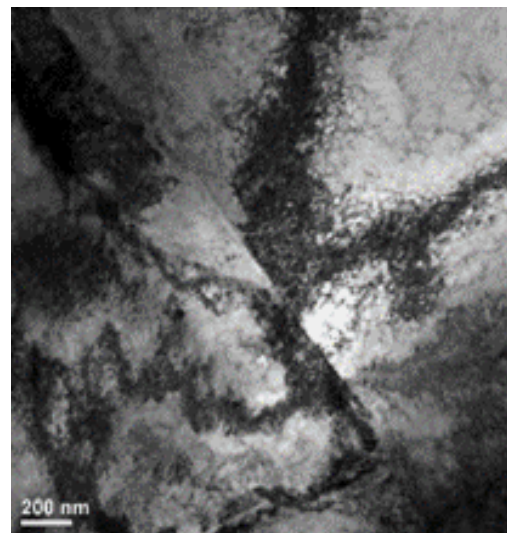
where  $\sigma_0$  is the initial yield stress of the material,  $\alpha$  is a material constant,  $G$  is the shear modulus,  $b$  is the Burgers vector, and  $\rho$  is the dislocation density. Substituting values of  $G=81\text{GPa}$  [15],  $b=2.536 \times 10^{-10}\text{m}$  [16] and  $\sigma_0 = 420\text{MPa}$  [15] into Eq. (5), the value of  $\alpha$  for the present Inconel 625 alloy is found to be 0.316.



(a)

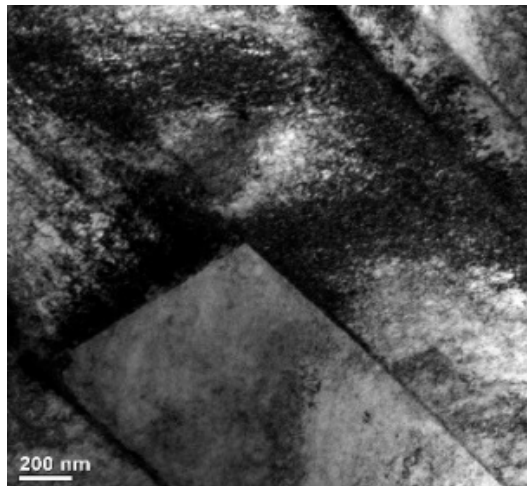


(b)

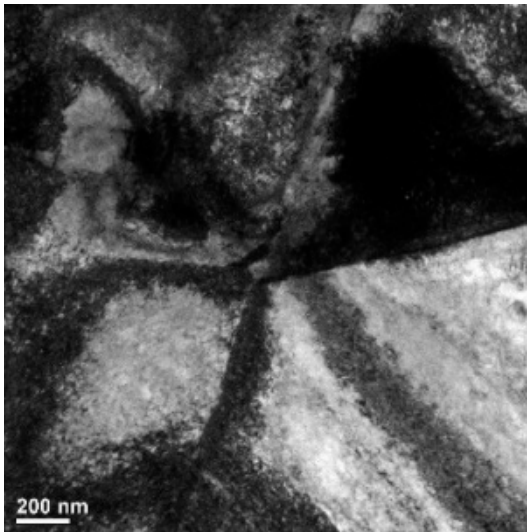


(c)

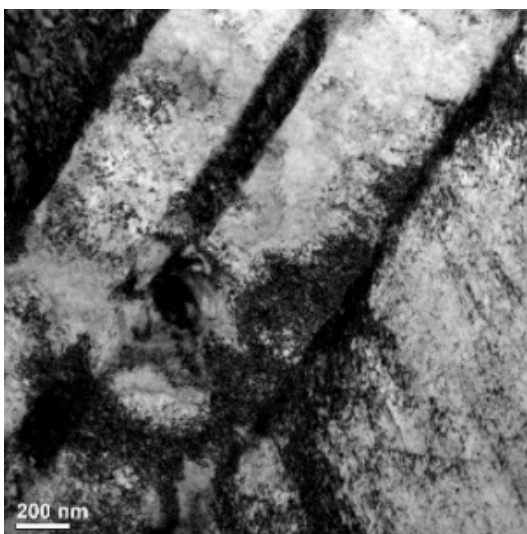
Figure 5: TEM micrographs showing dislocation microstructures of Inconel 625 specimens deformed at (a)  $3.7 \times 10^3 \text{ s}^{-1}$  and  $25^\circ\text{C}$ ; (b)  $6.4 \times 10^3 \text{ s}^{-1}$  and  $25^\circ\text{C}$ ; (c)  $3.7 \times 10^3 \text{ s}^{-1}$  and  $300^\circ\text{C}$ ;



(d)



(e)



(f)

Figure 5: TEM micrographs showing dislocation microstructures of Inconel 625 specimens deformed at (d)  $6.4 \times 10^3 \text{ s}^{-1}$  and  $300^\circ\text{C}$ ; (e)  $3.7 \times 10^3 \text{ s}^{-1}$  and  $750^\circ\text{C}$ ; and (f)  $6.4 \times 10^3 \text{ s}^{-1}$  and  $750^\circ\text{C}$ .

## CONCLUSION

Dynamic impact tests have been performed to investigate the effects of the strain rate ( $3700\sim 6400 \text{ s}^{-1}$ ) and temperature ( $25\sim 750^\circ\text{C}$ ) on the mechanical properties and dislocation substructure of Inconel 625 nickel-based super alloy. The results have shown that the stress-strain response of the specimens depends strongly on both the strain rate and the temperature. In particular, a strengthening effect is observed as the strain rate is increased or the deformation temperature is decreased. In addition, it has been shown that the stress and temperature dependence of the strain rate is adequately described by the Zener-Hollomon parameter ( $Z$ ). Finally, the TEM observations have shown that the dislocation density increases with increasing strain rate, but decreases with increasing temperature. The relationship between the dislocation density and the work hardening stress can be adequately described using the Bailey-Hirsch equation with a material constant of  $\alpha=0.316$ .

## ACKNOWLEDGMENT

The authors gratefully acknowledge the financial support provided to this study by the Ministry of Science and Technology (MOST) of Taiwan under Contract No. MOST 10-2221-E-006-072-MY3

## REFERENCES

- Davis J.R., "ASM specialty handbook: nickel, cobalt, and their alloys," ASM International, Member/Customer Service Center, Materials Park, OH 44073-0002, USA, 2000. 442, 2000.
- Dinda G.P., Dasgupa A.K., Mazumder J., "Laser aided direct metal deposition of Inconel 625 in long-term intermediate temperature applications," *International Journal of Pressure Vessels and Piping* 59 (1994) 98-104.
- Ehrlich K., Konys J., Heikinheimo, "Materials for high performance light water reactors," *Journal of Nuclear Materials* 327 (2004) 140-147.
- Ham R.K., "The determination of dislocation densities in thin films," *Phil. Mag.* 6 (1961) 1183-1184.
- Hodge F.G., "The history of solid-solution-strengthened Ni alloys for aqueous corrosion service," *JOM* 58 (2006) 28-31.
- Huang F., Tao. N. R., "Effects of Strain Rate and Deformation Temperature on Microstructures and Hardness in Plastically Deformed Pure Aluminum," *Journal of Materials Science & Technology* 27 (2011) 1-7.
- Ishikawa K., Watanabe H., Mukaib T., "High strain rate deformation behavior of an AZ91 magnesium alloy at elevated temperatures," *Mater. Lett* 59 (2005) 1511-1515.
- Jonas J.J., Sellars C.M., McG Tegart W.J., "Strength and structure under hot-working conditions," *Metall. Rev.* 14 (1969) 1-24.

- Lee W.S., Lin C.F., "Plastic deformation and fracture behaviour of Ti-6Al-4V alloy loaded with high strain rate under various temperatures," Mater. Sci. Eng. A 241 (1998) 48-59.
- Lee W.S., Lin C.F., Chen T.H., Chen H.W., "Dynamic mechanical behaviour and dislocation substructure evolution of Inconel 718 over wide temperature range," Mater. Sci. Eng. A 528 (2011) 6279-6286.
- Lee W.S., Liu C.Y., Chen T.H., Luo W.Z., "High temperature deformation and fracture behavior of 316L stainless steel under high strain rate loading," Mater. Sci. Eng. A 420 (2012) 226-234.
- Li. Y.S., Zhang Y., Tao. N. R., Lu K., "Effect of the Zener-Hollomon parameter on the microstructures and mechanical properties of Cu subjected to plastic deformation," Acta Mater. 57 (2009) 761-772.
- Shankar V., Bhanu Sankara Rao K., "Microstructure and mechanical properties of Inconel 625 superalloy," Journal of Nuclear Materials 288 (2001) 222-232.
- Sundararaman M, Mukhopadhyay P, and Banerjee S, "Precipitation of the  $\delta$ -Ni3Nb phase in two nickel base superalloys," Metall. Trans. A 19 (1988) 453-465.
- Tomota Y., Lukas P., Harjo S., Park J.H., Tsuchida N., Neov D., "In situ neutron diffraction study of IF and ultra low carbon steels upon tensile deformation," Acta Mater. 51 (2003) 819-830.
- Zener C., Hollomon J.H., "Effect of Strain Rate Upon Plastic Flow of Steel," Journal of Applied Physics (1944) 15-22.

## 鎳基超合金Inconel625撞擊下之高溫變形行為與差排結構分析

李偉賢 黃建璋  
國立成功大學機械工程系

### 摘要

鎳基超合金Inconel 625具有優異的機械及物理性能，已被廣泛應用在航太、交通、與飛彈之應用。本研究利用哈普金森高速撞擊試驗機，研究Inconel 625鎳基超合金在高速撞擊下之高溫變形行為。撞擊之應變速率控制 $3.7 \times 10^3 \sim 6.4 \times 10^3 \text{ s}^{-1}$ 之間，溫度分別為 $25^\circ\text{C}$ 、 $300^\circ\text{C}$ 與 $750^\circ\text{C}$ 。結果顯示，應變速率及溫度對Inconel 625鎳基超合金之高溫變形行為有重要之影響。其強度及加工硬化速率隨著應變速率的上升而上升，但隨溫度之上升而下降。而應變速率與溫度在高溫變形行為上的耦合效應可由Zener-Hollomon參數準確地描述。微觀結構分析指出，差排密度隨著應變速率的上升而增加，但隨溫度之上升而衰減。其與加工硬化強度之間的關係可藉由Bailey-Hirsch 方程式 $\sigma = \sigma_0 + \alpha_1 G b \sqrt{\rho}$ 來完整的描述，其中 $\alpha_1 = 0.316$ 。